This is a repository copy of *Elastic-plastic response of plates subjected to cleared blast loads*.

Elastic-plastic response of plates subjected to cleared blast loads

S.E. Rigby[a,*], A. Tyas[a], T. Bennett[b]

[a]*Department of Civil & Structural Engineering, University of Sheffield, Mappin Street, Sheffield, S1 3JD, UK*
[b]*School of Civil, Environmental & Mining Engineering Engineering, North N136, North Terrace Campus, The University of Adelaide, SA 5005, Australia*

Abstract

A commonly used approach for the engineering analysis of structures subjected to explosive loads is to approximate the problem as an equivalent Single-Degree-of-Freedom (SDOF) system and to use elastic-plastic response spectra. Currently, the response spectra that exist in the literature do not take into account the fact that blast wave clearing will occur if the target is not part of a reflecting surface that is effectively infinite in lateral extent. In this article, response spectra for equivalent SDOF systems under cleared blast loads are obtained by solving the equation of motion using the linear acceleration explicit dynamics method, with the clearing relief approximated as an acoustic pulse. The charts presented in this article can be used to predict the peak response of finite targets subject to explosions, and are found to be in excellent agreement with a finite element model, indicating that the response spectra can be used with confidence as a first means for predicting the likely damage a target will sustain when subjected to an explosive load. Blast wave clearing generally serves to reduce the peak displacement of the target, however it is shown that neglecting clearing may be unsafe for certain arrangements of target size, mass, stiffness and elastic resistance.

Keywords: Blast, Clearing, Elastic-plastic, Response spectra, SDOF

[*]Tel.: +44 (0) 114 222 5724
 Email address: `sam.rigby@shef.ac.uk` (S.E. Rigby)

Nomenclature

A	-	panel area
b	-	waveform parameter (decay of exponential pressure time curve)
c	-	damping coefficient
d	-	thickness
E	-	Young's Modulus
F	-	force
F_e	-	equivalent force
$F_{e,max}$	-	peak equivalent force
$F_{e,min}$	-	peak negative phase equivalent force
H	-	scaled target height
i_r	-	reflected positive phase specific impulse
I	-	second moment of area
k	-	stiffness
k_e	-	equivalent stiffness
K_L	-	load factor
K_M	-	mass factor
K_S	-	spatial load factor
L	-	span
m	-	mass
m_e	-	equivalent mass
M_m	-	moment capacity at mid-span
p	-	pressure
$p_{r,max}$	-	peak reflected pressure
R	-	range from charge centre (stand-off),
R_u	-	elastic resistance
t	-	time
t_a	-	time of arrival of blast wave
t_d	-	positive phase duration
t_d^-	-	negative phase duration
$t_{d,lin}$	-	positive phase duration (linear approximation)
T	-	natural period
W	-	explosive mass
x	-	length along beam
z	-	displacement
z_E	-	elastic limit
z_{max}	-	peak displacement
$z_{max,inf}$	-	peak displacement under exponential (non-cleared) load
$z_{max,lin}$	-	peak displacement under linear load
$\dot{z}$	-	velocity
$\ddot{z}$	-	acceleration
Z	-	scaled distance ($R/W^{1/3}$)
ρ	-	density
σ_y	-	yield strength
ϕ	-	normalised deflected shape

1. Introduction

The intense loading produced from a high explosive detonation can cause significant damage to structural elements, potentially resulting in failure, structural collapse and loss of life. In order to best protect civilian and military infrastructure from explosions, it is important to understand and be able to predict the performance of key components subjected to blast loads.

Numerical analysis methods can be used to model the dynamic response of structures subjected to explosive loads. Finite element (FE) simulations, for example, can model the detonation process, blast wave propagation through air and subsequent interaction with the target [1, 2, 3, 4], as well as complex geometries and material nonlinearities [5, 6]. Whilst these methods often produce results that are in excellent agreement with experimental observations, high levels of complexity and long analysis times often render such simulations unsuitable, especially during the early stages of design.

Alternative analysis methods may be used, particularly when assessing the approximate level of damage a target will sustain before more refined analyses are undertaken. The Unified Facilities Criteria Design Manual (UFC-3-340-02), *Structures to Resist the Effects of Accidental Explosions* [7], recommends the use of the equivalent Single-Degree-of-Freedom (SDOF) method [8]. The SDOF method is often favoured because of its ease of use, relatively few input requirements and available guidance in the literature [7, 9, 10], and is usually presented as design charts in the form of response spectra.

In these response spectra, the peak dynamic displacement of the target can be obtained from knowledge of the magnitude of the applied load and the ratio of the load duration to response time of the target. These charts were first produced by Biggs [8] and are based on the assumption of a linearly decaying blast load, rather than the exponential 'Friedlander' decay used in the well-established empirical load prediction method of Kingery and Bulmash [11] and ConWep [12]. This limitation has been addressed by Gantes and Pnevmatikos [13], where response spectra are provided for exponential loading, under the assumption that the target is part of a reflecting surface that is infinite in lateral extent.

In the case of reflecting surfaces that cannot be said to be infinite, it is well known that blast wave clearing can significantly reduce the late-time pressure acting on the target face [14, 15, 16, 17], reducing the total reflected impulse by up to 50% [18, 19]. The influence of clearing on the response of elastic targets subjected to blast loads has recently been investigated by the current authors [20, 21], however the effect of target plasticity remains un-quantified. The purpose of this paper is two-fold: firstly, to develop a complete set of response spectra for finite targets subjected to blast loads, and secondly, to compare these spectra to existing guidance to quantify the effect of blast wave clearing.

2. Elastic-plastic SDOF systems

2.1. The SDOF method

The dynamic equation of motion of a distributed system, for example a simply supported beam with a transiently varying, spatially uniform load (as in Figure 1) is given as

$$m\ddot{z} + c\dot{z} + kz = F(t), \tag{1}$$

where m, c and k are the mass, damping and stiffness of the system, $\ddot{z}$, $\dot{z}$ and z are the acceleration, velocity and displacement, and $F(t)$ is the externally applied force. The equivalent SDOF method 'transforms' the distributed properties of the real life system into equivalent single-point properties, where the displacement of the single-degree system is equated to the point of maximum displacement in the distributed system, i.e. displacement at midspan of a simply supported beam.
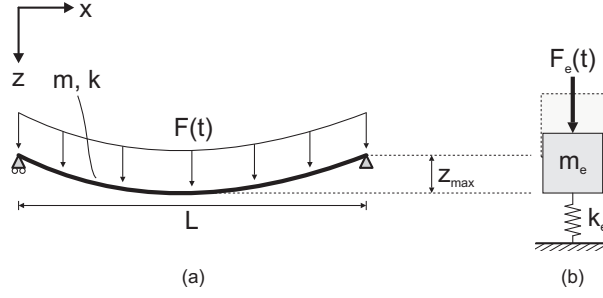
Figure 1: (a) Distributed and (b) equivalent SDOF systems

Ignoring damping, the dynamic equation of motion of the equivalent system is

$$m_e \ddot{z}(t) + k_e z(t) = F_e(t),$$
(2)

where m_e, k_e and $F_e(t)$ are the equivalent mass, stiffness and force. Equating the work done, kinetic energy and internal strain energy of the two systems, the dynamic equation of motion for the SDOF system now becomes

$$K_M m\ddot{z} + K_L kz = K_L F(t).$$
(3)

where the mass factor, K_M, and load factor, K_L, are used to transform the distributed properties into the single point equivalent values. The transformation factors for various support conditions and loading distributions, based on the assumption of the normalised deflected shape, ϕ, can be found in the literature [7, 8, 9, 10].

2.2. Elastic-plastic response spectra

In the analysis performed by Biggs [8], elastic-plastic SDOF systems are subjected to a linearly decaying uniform load

$$F_e(t) = \begin{cases} F_{e,max}\left(1 - \dfrac{t}{t_{d,lin}}\right), & t \leq t_{d,lin} \\ 0, & t > t_{d,lin} \end{cases}$$
(4)

where $F_{e,max}$ is the peak force and $t_{d,lin}$ is the duration of the triangular load. The SDOF system has a bilinear elastic-perfectly plastic resistance function as shown in Figure 2. This comprises linear elastic behaviour with spring resistance $k_e z$ until the elastic limit, z_E, is reached, followed by plastic behaviour with constant spring resistance, R_u, thereafter. After the peak displacement, z_{max}, is reached, the displacement decreases and the system begins to rebound. When rebounding, the system again behaves elastically until a spring force of $-R_u$ is attained, whereby the system returns to plasticity.

In this article, the equation of motion (3) is solved using the linear acceleration method [8]. Typically, it is only the peak displacement that is of interest to the engineer – by varying the ratio of $R_u/F_{e,max}$, and the ratio of $t_{d,lin}/T$, where T is the natural period of the target

$$T = 2\pi \sqrt{\frac{m_e}{k_e}},$$
(5)

the response spectra of elastic-plastic SDOF systems subjected to triangular loads can be presented, as in Figure 3, where the peak response is normalised against the elastic limit, i.e. z_{max}/z_E. Providing the mass, stiffness,
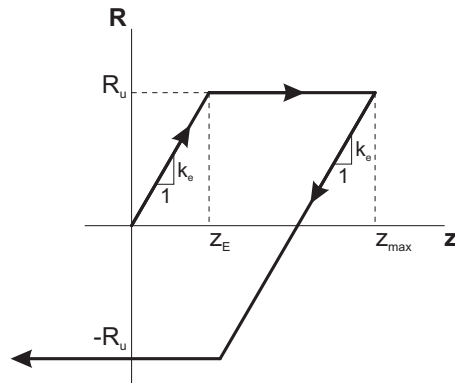
4

Figure 2: Resistance-deflection function of an Elastic-Plastic SDOF system

resistance and load-time history are known, the peak displacement can be read from the response spectra. The time ratio, t_d/T, gives an indication of the response time of the target with respect to the load duration – low values of time ratio indicate impulsive conditions where the loading is completed during the early stages of displacement, whereas high values of time ratio indicate quasi-static conditions where the target can be expected to reach peak displacement long before the loading is complete.
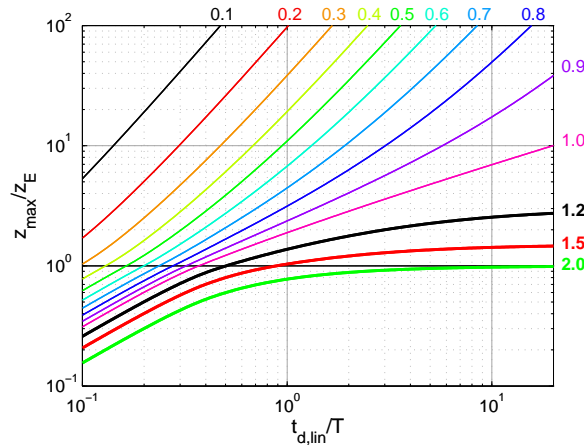

Figure 3: Maximum deflection and of an elastic-plastic SDOF System under a triangular load (after Biggs [8]). Numbers next to curves are $R_u/F_{e,max}$

3. Elastic-plastic response to exponential blast loads

A more accurate description of blast pressure-time history is an exponential decay from peak pressure, $p_{r,max}$, to ambient pressure at time t_d (known as the positive phase duration). Following this is a period of 'negative'

(below atmospheric) pressure known as the negative phase, the duration of which is given as $\bar{t}_d$. This is shown schematically in Figure 4. The positive phase can be described by the 'modified Friedlander Equation' [22],

$$p(t) = p_{r,max}\left(1 - \frac{t}{t_d}\right)e^{-bt/t_d},$$ (6)

where b is the coefficient that describes the rate of decay of the pressure-time curve.
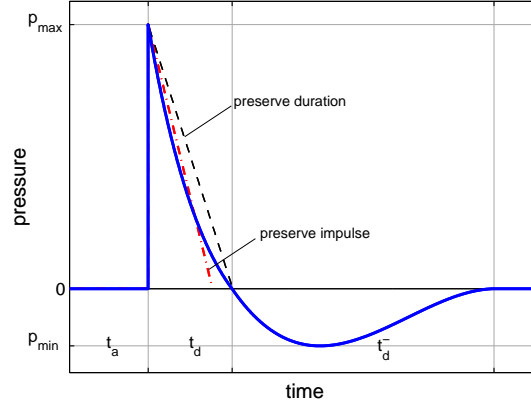

Figure 4: Exponential pressure-time profile for a blast wave with triangular approximations of the positive phase

The triangular load model does not capture the correct decay of the pressure-time curve and it neglects the negative phase. Teich and Gebekken [23] and Krauthammer and Altenberg [24] have shown this to be an inaccurate assumption, particularly if the scaled distance is large. Gantes and Pnevmatikos [13] address this limitation by providing response spectra for exponential loading where the Friedlander equation (6) is simply extended to $t \to \infty$ to capture the negative phase and compare this to the triangular response spectra of Biggs. In the current study, the negative phase is modelled using the cubic expression from the Naval Facilities Engineering Command manual *Blast Resistant Structures* [25], as this has shown to be in better agreement with experimental observations [20]. The piecewise force-time function applied to the SDOF model is given in equation 7

$$F_e(t) = \begin{cases} F_{e,max}\left(1 - \frac{t}{t_d}\right)e^{-bt/t_d}, & t \leq t_d \\ F_{e,min}\left(\frac{6.75(t - t_d)}{t_d^-}\right)\left(1 - \frac{(t - t_d)}{t_d^-}\right)^2, & t_d < t \leq t_d + t_d^- \\ 0, & t > t_d + t_d^- \end{cases}$$ (7)

where $F_{e,max}$ and $F_{e,min}$ are given by the peak overpressure and peak negative pressure multiplied by the target area and load transformation factor. These parameters, along with the positive phase duration, t_d, negative phase duration, $\bar{t}_d$, and waveform parameter, b, are found using the Kingery and Bulmash [11] empirical predictive method. This method is based on curves fit to a database of experimental records of blast loading parameters from a wide range of explosive events, and forms the core of the widely used blast loading predictive tool ConWep [12]. Given the scaled distance, $Z = R/W^{1/3}$, where R is the distance from the point of interest to the charge

6

centre (called the range or stand-off) and W is the mass of explosive, expressed as an equivalent mass of TNT, the relevant blast parameters can be read and used to construct the applied blast pressure-time history.

Figure 5 shows as an example the response spectrum for an elastic-plastic SDOF system under an exponential blast load at $Z = 8$ m/kg$^{1/3}$ and $R_u/F_{e,max} = 0.5$. The triangular response spectrum is also shown, with $t_{d,lin} = 2i_r/p_{r,max}$ to preserve positive phase impulse (Figure 4). Dashed regions of the exponential response spectrum indicate regions where the peak displacement is in rebound.
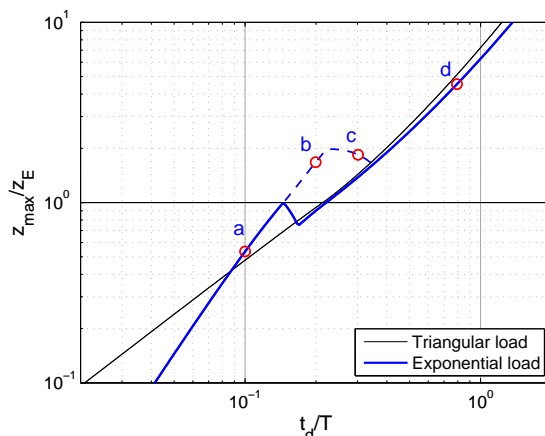

Figure 5: Response spectra for $Z = 8$ m/kg$^{1/3}$ and $R_u/F_{e,max} = 0.5$ under triangular and exponential loads. Peak displacements from the examples in Figure 6(a-d) are shown with corresponding values of t_d/T

With reference to Figure 5, the exponential load response spectrum for $R_u/F_{e,max} = 0.5$ is defined by four distinct regions:

a. Elastic deformation only, $t_d/T < 0.15$

Figure 6(a) shows the SDOF response at $t_d/T = 0.1$ (force-time history shown on the minor y axis). In this region of the response spectrum, $z_{max} < z_E$ and no plastic deformation occurs. As the system reaches peak displacement on the first cycle, the velocity of the system becomes negative whilst the negative phase load is still applied, increasing deflection in the negative ('rebound') direction and causing the peak displacement to occur during rebound. This behaviour continues with increasing values of t_d/T until the rebound is sufficient to cause plasticity in the negative direction.

b. Plastic deformation in rebound only, $0.15 \leq t_d/T < 0.22$

Figure 6(b) shows the SDOF response at $t_d/T = 0.2$. It can be seen that the only permanent plastic deformation is in the negative direction, i.e. towards the blast. As the ratio of t_d/T increases, the magnitude of positive displacement on the first cycle increases until the elastic limit is reached.

c. Plastic deformation in both directions, $0.22 \leq t_d/T < 0.35$

Figure 6(c) shows the SDOF response at $t_d/T = 0.3$. The system undergoes plastic deformation on the first positive cycle of displacement and undergoes further plastic deformation in rebound. The system still reaches peak displacement in rebound in this region of the response spectrum, with the positive plastic deformation increasing relative to the negative with increasing t_d/T.

d. Peak plastic deformation during the first half cycle of displacement, $t_d/T \geq 0.35$

Figure 6(d) shows the SDOF response at $t_d/T = 0.8$. The positive phase of the load is sufficient to cause gross plastic deformation ($z_{max} \gg z_E$). Little or no rebound plasticity occurs.
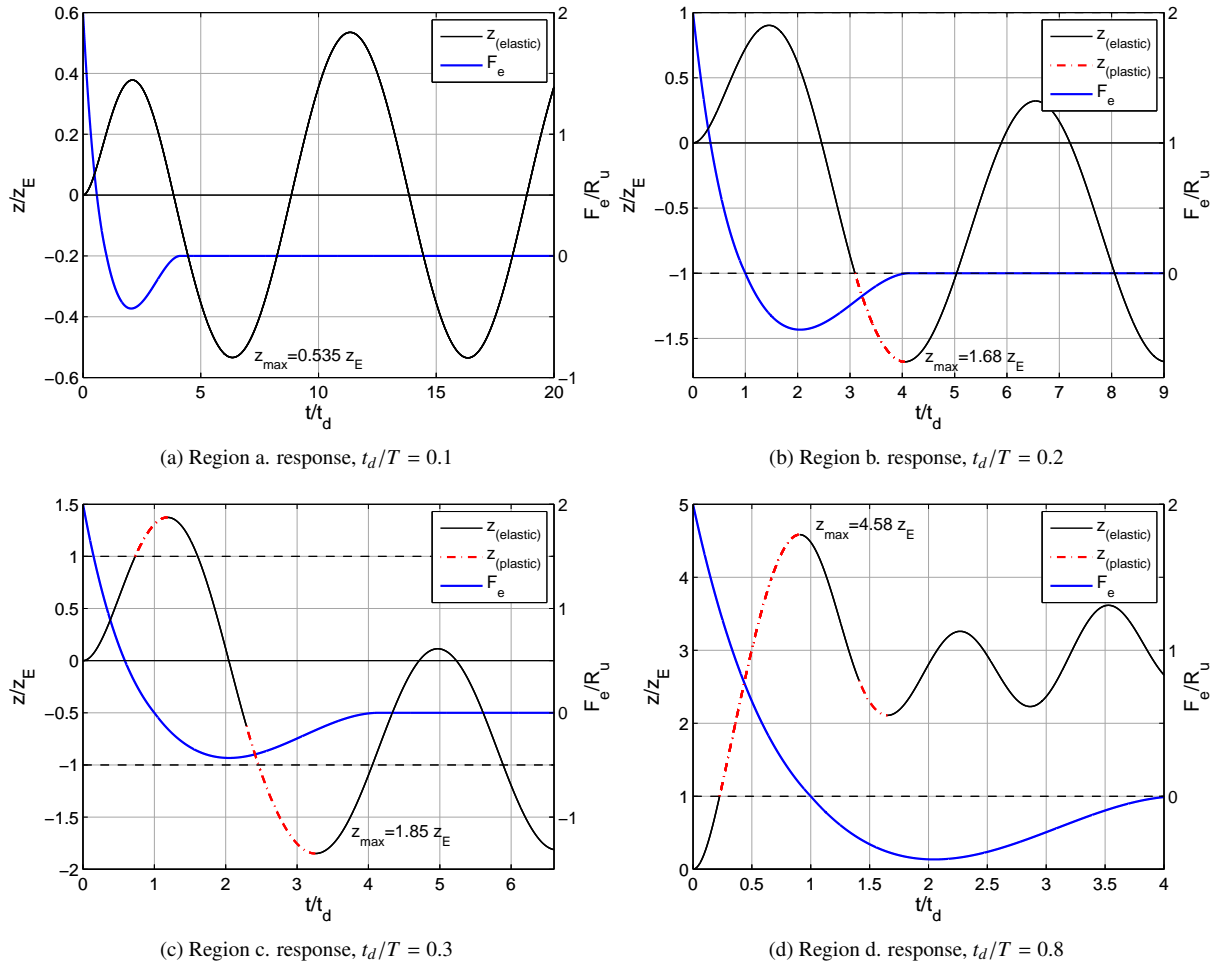
Figure 6: Normalised displacement-time history of elastic-plastic SDOF systems under an exponential blast load at $Z = 8 \text{ m/kg}^{1/3}$

The discontinuities in the response spectrum are caused by the transitions between these regions. Whilst the bounds of each region will change with different values of $R_u/F_{e,max}$, the behaviour within each region will be similar.

By comparing the triangular and exponential response spectra, it is apparent that the loading assumption has a significant impact on the response of the SDOF system, and that the triangular load model is over-conservative for impulsive scenarios (low values of t_d/T). The triangular load model is also non-conservative for particular ranges of t_d/T where the exponential load response spectrum is in regions b. and c. and peak displacement occurs during rebound.

8

4. Elastic-plastic response to cleared blast loads

The assumption of an exponential 'Friedlander' decay, however, is only valid if the target is part of a reflecting surface that is large in dimensions perpendicular to the direction of travel of the blast wave. When a blast wave reaches the edge of a finite target, diffraction of the shock front around the target edge causes an expansion wave to travel inwards along the loaded face. This expansion wave reduces the pressure acting at any point that the wave propagates over in a process known as blast wave clearing.

Current methods for treating blast wave clearing that exist in design guidance [7, 12] cannot account for early negative pressures associated with blast wave clearing, an effect which has been shown both experimentally [14, 15, 16, 17] and numerically [19, 26], and can increase peak displacement when it coincides with target rebound [20].

The Hudson method [27], based on approximation of the relief wave as an acoustic pulse, enables blast wave clearing to be predicted to a high level of accuracy [14, 20] and forms the basis of the numerical analysis in this study. The dimensionless formulation of the Hudson method ensures that, for a given value of Z, any target with the same scaled height $H = L/W^{1/3}$ will be subjected to the same distribution of pressure regardless of the span, L. Henceforth the dimensionless ratio of Z/H is used to indicate target size.

The distribution of blast pressure, $p(x, y, t)$, that arises from blast wave clearing is given by discretising the target into 100×100 nodes and applying the Hudson clearing corrections to the ConWep reflected pressure-time history at each point. The distribution of pressure is converted into a uniform pressure at each time step using the time-varying spatial load factor, K_S [20], such that

$$F_e(t) = K_L K_S(t) F(t), \tag{8}$$

where $F(t)$ is the *total* force acting on the plate and $F_e(t)$ is the energy equivalent load that takes into account both the standard SDOF load transformation *and* the non-uniformity of the load.

The spatial load factor is given such that the non-uniform load acting on the assumed deflected shape, ϕ, has the same work done as an equivalent uniform load,

$$K_S(t) = \frac{\int_A p(x, y, t) \phi(x, y) \, dA}{\int_A p(x, y, t) \, dA \int_A \phi(x, y) \, dA}, \tag{9}$$

where the expression is numerically integrated over A, the panel area. It is assumed that the panel deforms in the first mode of vibration only, i.e. that the blast pressure distribution changes sufficiently quickly to not influence the deformation *profile* of the panel, which has been shown to be valid through finite element analysis [20] and experimental work [21]. The normalised deflected shape of a simply supported beam under a uniform load is given as

$$\phi(x) = \frac{16x}{5L^4} \left(L^3 - 2Lx^2 + x^3 \right), \tag{10}$$

where x is the length along the beam and L is the total length. For a one-way spanning member, $\phi(x, y) = \phi(x)$.

Figure 7 shows the normalised equivalent force acting on simply supported, one-way spanning square plates of different scaled target size. $Z/H = 0$ indicates a target that can be assumed to be infinite in lateral extent and is subjected to the full reflected pressure for the entire duration of loading.

Response spectra for $Z = 8$ m/kg$^{1/3}$ and $Z/H = 0, 4, 8$ and 16 are shown in Figures 8(a-d) respectively, showing the peak response of elastic-plastic SDOF systems subjected the normalised cleared forces shown in Figure 7. Response spectra for $Z = 2, 4$ and 16 m/kg$^{1/3}$ are provided in the Appendix.

9
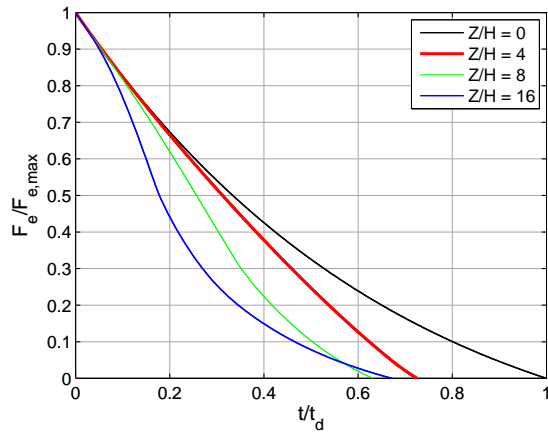
(a)
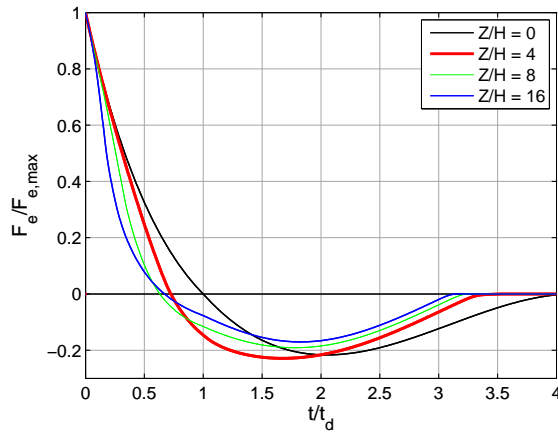
(b)

Figure 7: Normalised force-time acting on finite targets of differing size, (a) positive phase only, (b) entire duration

5. Discussion

5.1. The influence of scaled distance and target size

Rose and Smith [19] and Tyas et al. [14] observed an increasing significance of clearing with larger scaled distances. Table 1 shows the comparison of peak displacements under the non-cleared blast load for $H = \infty$ and the cleared blast load for $H = 1$, over a range of resistance ratios and time ratios. The results are in agreement with this observation of more complete clearing occurring at increased distance from the blast source – the difference
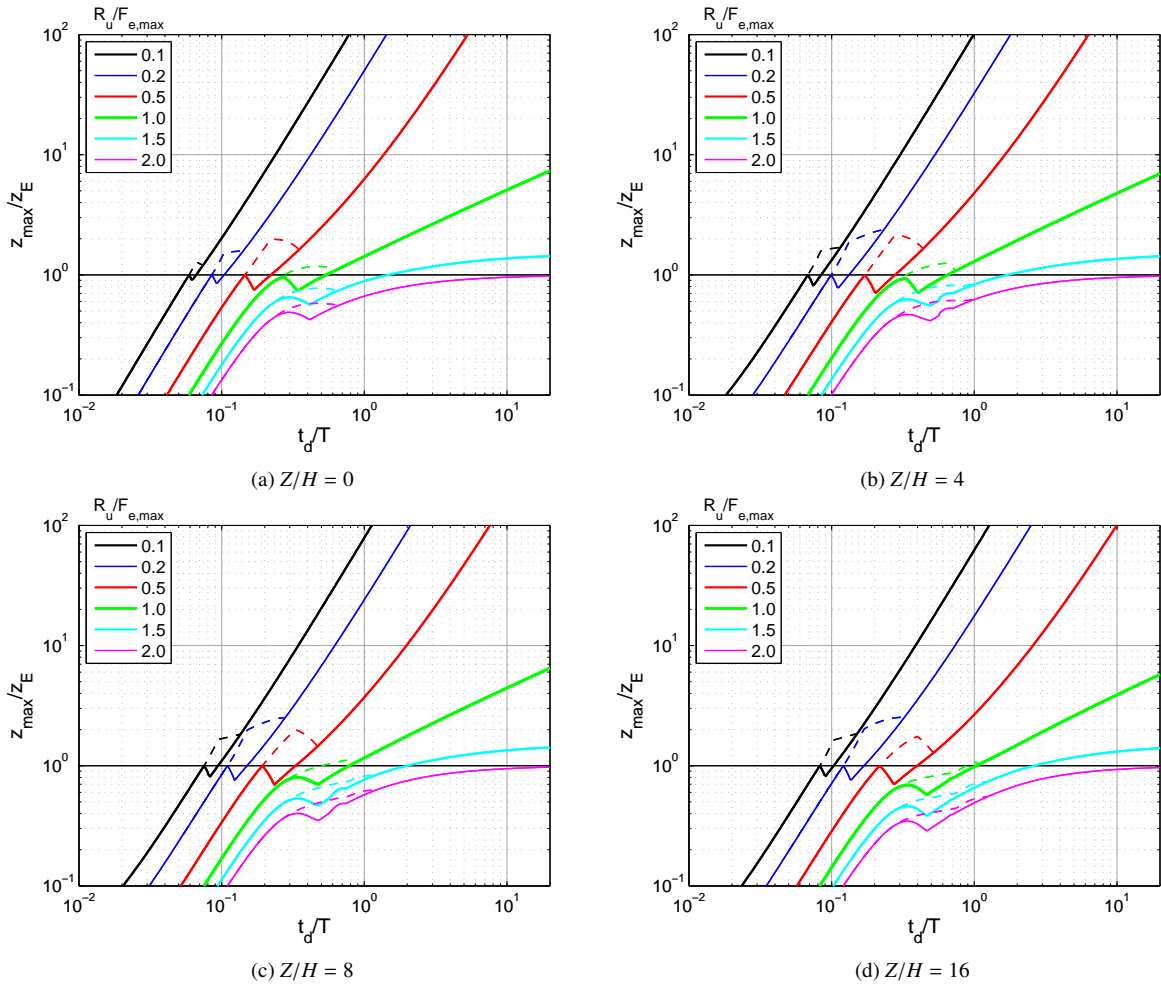
(a) $Z/H = 0$

(b) $Z/H = 4$

(c) $Z/H = 8$

(d) $Z/H = 16$

Figure 8: Response spectra for $Z = 8$ m/kg$^{1/3}$. Dashed lines indicate regions where the peak displacement is in rebound

in response due to the non-cleared and cleared blast load is greater in almost every case at $Z = 16$ when compared to $Z = 4$.

From inspection of Figure 8, it is also apparent that the rebound regions of the response spectra (regions b. and c., as indicated by the dashed lines) are larger for smaller scaled target sizes. This can be justified by the fact that as the expansion wave propagates over the target face, the magnitude of the relief pressure decreases and the pressure pulse becomes more rounded and longer in duration [27]. With smaller targets, therefore, a sharper drop-off in pressure occurs more uniformly across the loaded face, making smaller targets more susceptible to the dynamic effects that cause increased displacement in rebound.

11

$R_u/F_{e,max}$	t_d/T	z_{max}/z_E					
		Z = 4			Z = 16		
		$H = \infty$	$H = 1$	% diff.	$H = \infty$	$H = 1$	% diff.
0.2	0.2	1.96	1.66	15	2.75	3.32	-21
	0.5	8.78	4.91	44	13.9	6.69	52
	1.0	31.1	17.0	45	51.2	22.2	57
0.5	0.2	1.09	0.71	34	1.90	1.19	37
	0.5	1.68	1.27	25	2.59	1.82	30
	1.0	3.83	2.87	25	6.62	3.40	49
1.0	0.2	0.54	0.36	34	0.84	0.59	30
	0.5	0.84	0.83	1	1.35	1.03	24
	1.0	1.14	1.07	6	1.46	1.11	24

Table 1: Comparison of peak displacement for $H = \infty$ and $H = 1$ at $Z = 4$ and $Z = 16$

5.2. Comparison against exponential and triangular load response spectra

A number of observations on the influence of clearing can be made when the cleared response spectra are compared with the triangular load response spectra. Figure 9 shows the spectra for $R_u/F_{e,max} = 0.5$ from Figures 8(a-d), as well as the linear load response spectrum from Figure 3. Towards the impulsive end of the response spectra (low values of t_d/T), the reduction in net impulse associated with clearing and the negative phase can be seen to significantly reduce the peak displacement of the SDOF system under the cleared load relative to the triangular load. The influence of target size can be seen to further reduce peak displacement. For example, at $t_d/T = 0.2$, the displacement of the cleared plate with $Z/H = 16$ is $0.9z_E$, whereas the displacement under the exponential load ($Z/H = 0$) is $1.7z_E$. Furthermore, the peak displacement under the cleared load at $Z/H = 16$ is around 33% of the peak displacement under the exponential load at large values of t_d/T. Clearing is therefore an important consideration for elastic-plastic systems, even at large values of t_d/T where it is unimportant for elastic systems [20].
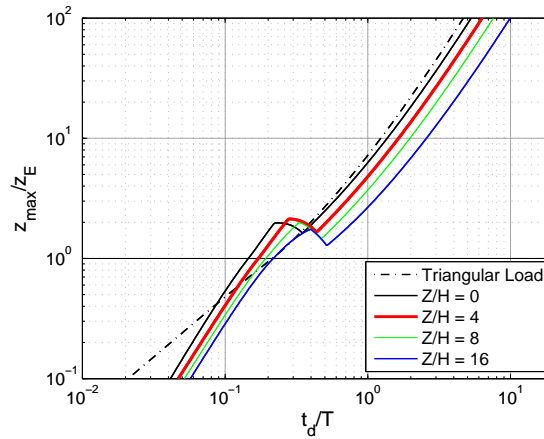

Figure 9: Response spectra for $Z = 8$ m/kg$^{1/3}$ and $R_u/F_{e,max} = 0.5$ for different scaled target sizes, normalised against elastic limit

Figure 10(a) shows contours of peak displacement, z_{max}, normalised against the peak displacement of the SDOF under the triangular load, $z_{max,lin}$. The dashed line indicates the time ratio at which the system begins deform plastically (i.e. when $z_{max}/z_E > 1$ in Figure 8), with elastic behaviour to the left and plastic behaviour to the right of the curve. It can be seen that peak values of displacement occur between $0.3 < R_u/F_{e,max} < 0.7$, when the system undergoes plastic deformation in rebound only. Figure 10(b) shows the normalised response spectra at select values of $R_u/F_{e,max}$. If the temporal characteristics of the loading relative to the response of the target are such that greater displacement is caused in rebound ($t_d/T \approx 0.25$), and the resistance of the target is such that it enters plasticity in rebound (as, for example $R_u/F_{e,max} = 0.5$), then an amplification in displacement will occur.

It is apparent that blast wave clearing can serve to adversely affect target response when the magnitude of load is comparable to the resistance of the target, and can serve to severely lessen the peak displacement when the magnitude of load far exceeds the elastic resistance. For elastic SDOF systems subjected to cleared blast loads, $R_u/F_{e,max} \geq 2.0$, the normalised response spectra approach 1.0 as t_d/T increases [20] [1]. Elastic-plastic systems, however, experience gross plastic deformation at higher time ratios (region d. of the response spectra) and hence the time taken to reach peak displacement increases, allowing time for the effects of clearing to decelerate the SDOF system.

5.3. The influence of clearing

Normalising the peak displacement of the SDOF under the cleared load against the peak displacement of the SDOF under the exponential load, $z_{max,inf}$, as in Figure 11(a), allows the influence of clearing to be isolated and further quantified. The assumption that blast wave clearing is beneficial is clearly not always a valid or conservative assumption to make. For the elastic response spectrum there is a region between $0.47 < t_d/T < 0.80$ where 'clearing resonance' occurs and peak displacement is in the order of 10% greater than the SDOF under the full reflected pressure [20]. When plasticity is included in the model, this resonance can cause displacements over 25% greater than if clearing were neglected. Figure 11(b) shows an expanded view of the adverse region (note the linear x-axis), which can be seen to occur at time ratios as low as 0.2. Whilst it requires specific conditions for this to occur, it is worth noting that the phenomenon exists and blast wave clearing should not be neglected on the assumption that it is conservative.

The influence of clearing is complex and dependant on many parameters, however the response spectra presented in this article provide an effective method for quantifying this effect.

6. Application

The following section details the practical application of the response spectra using numerical and graphical examples and compares the results to both an explicit FE model and current design methods.

A square, simply supported, one-way spanning light cladding panel, shown schematically in Figure 12 – with Young's Modulus, $E = 65$ GPa, Density, $\rho = 2000$ kg/m^3 and Yield strength, $\sigma_y = 20$ MPa – is subjected to a 1 kg hemispherical TNT burst at a distance of 8 m. The panel has a span, L, of 1 m and thickness, d, of 10 mm. The dynamic SDOF properties of the panel, i.e. the equivalent mass, equivalent stiffness, elastic resistance, elastic limit and natural period, are determined using expressions shown in equations 11-15, after Biggs [8]
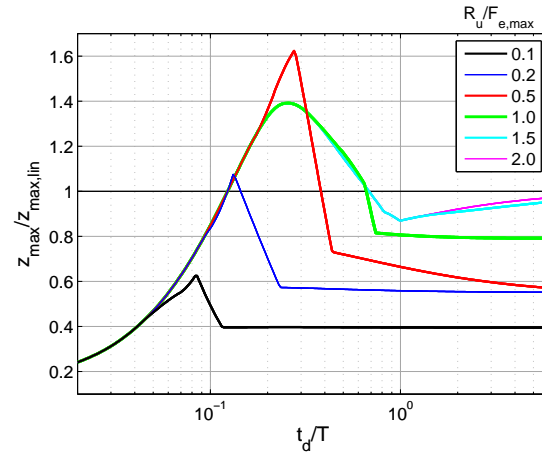
$$m_e = K_M \rho L^2 d \tag{11}$$

---

[1]When t_d/T is large, the natural frequency of the system is sufficiently high to ensure that the target reaches its peak displacement before the onset of clearing, i.e. there is no difference between the triangular, full reflected and cleared blast load, hence clearing has no effect.
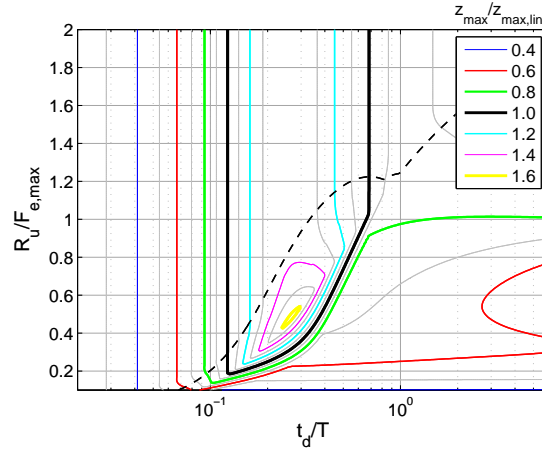
(a)

(b)

Figure 10: (a) Contours of peak displacement normalised against peak displacement under the triangular load for $Z = 8$ m/kg$^{1/3}$ and $Z/H = 4$. The dashed line indicates the time ratio at which the system begins to deform plastically. (b) Response spectra for select values of $R_u/F_{e,max}$
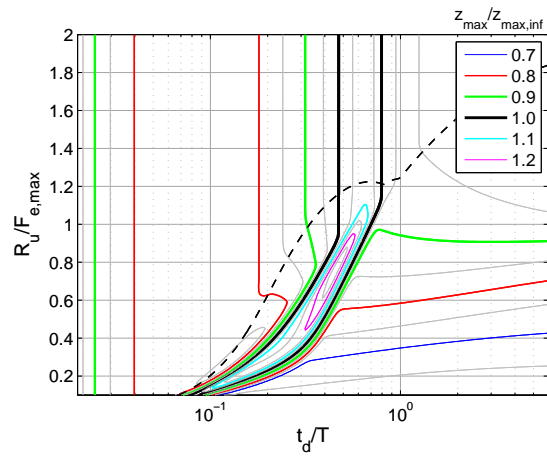
$$k_e = K_L 384EI/5L^3 \qquad (12)$$
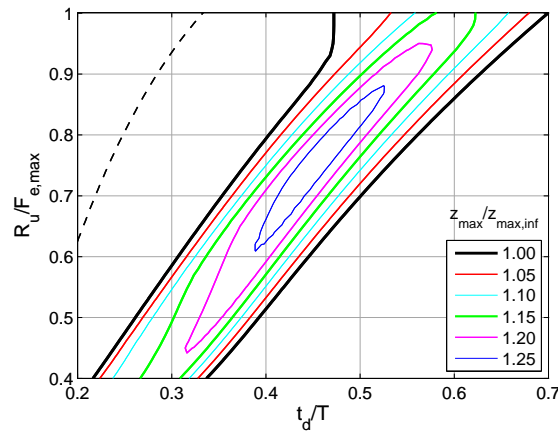
$$R_u = 8M_m/L \qquad (13)$$

$$z_E = R_u/k_e \qquad (14)$$

$$T = 2\pi \sqrt{m_e/k_e} \qquad (15)$$

where I is the second moment of area and M_m is the moment capacity at midspan. Elastic load and mass

14

(a)

(b)

Figure 11: Contours of peak displacement normalised against peak displacement under the exponential load for $Z = 8$ m/kg$^{1/3}$ and $Z/H = 4$, (a) entire region, (b) expanded view of adverse region. The dashed line indicates the time ratio at which the system begins to deform plastically

factors ($K_L = 0.64$, $K_M = 0.50$) are used as response is assumed to be predominantly elastic. The relevant loading parameters and dynamic properties are summarised in Table 2.

The SDOF equation of motion was solved for three load cases;

- 'Cleared' – blast load for $Z/H = 8$

- 'Exponential' – blast load for reflected pressure on an infinite surface, $Z/H = 0$

- 'Triangular' – linear decaying force with the same peak force and positive phase impulse as the exponential
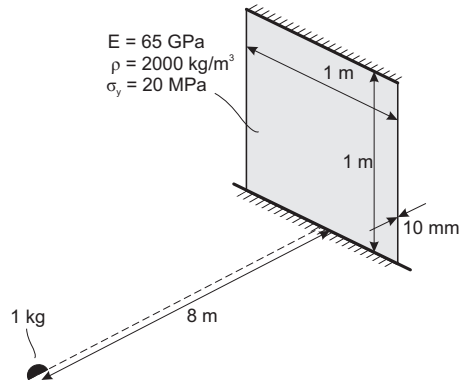
Figure 12: Dimensions and properties of the light cladding panel

Parameter	Symbol	Value (unit)
Peak reflected pressure	$p_{r,max}$	44.11 (kPa)
Positive phase duration	t_d	4.454 (ms)
Young's modulus	E	65 (GPa)
Density	ρ	2000 (kg/m^3)
Yield strength	σ_y	20 (MPa)
Load factor	K_L	0.64 (-)
Mass factor	K_M	0.50 (-)
Span	L	1 (m)
Thickness	d	10 (mm)
Equivalent stiffness	k_e	266.2 (kN/m)
Equivalent mass	m_e	10 (kg)
Elastic resistance	R_u	2.67 (kN)
Elastic limit	z_E	10.01 (mm)
Natural period	T	38.5 (ms)
Time ratio	t_d/T	0.116 (-)
Resistance ratio	$R_u/F_{e,max}$	0.094 (-)

Table 2: Loading parameters and dynamic properties for a 1×1 m elastic-plastic, one way spanning, simply supported panel.

load.

For the FE analysis, the panel was discretised using 100×100 shell elements using the *MAT_PLASTIC_KINEMATIC material model in LS-DYNA [28], with the cleared loading applied as force-time curves at every node using the method detailed in [21]. The Hudson method has been shown to accurately capture the spatial variation of cleared blast pressure loading [14] and can, when combined with an FE model, predict the dynamic deflection of finite plates to a good level of agreement with experimental results [21]. The FE model can therefore be considered as an accurate representation of how the panel would perform in real life.

Figure 13 shows the transient displacement of the SDOF models and FE simulation, with the bottom & left axes showing the real displacement-time history and the top & right axes showing the normalised history. The values of peak displacement are summarised in Table 3, where it can be seen that the peak SDOF displacement

16

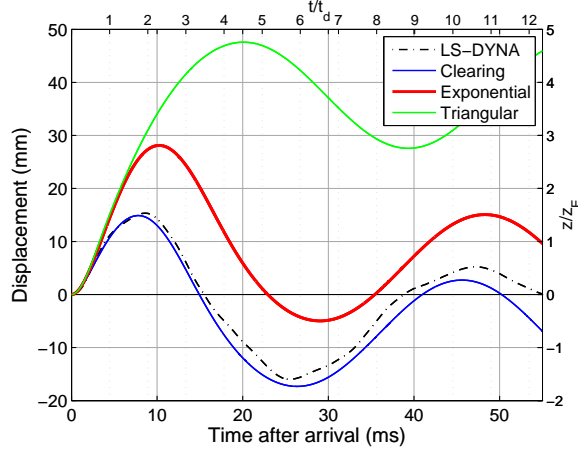under the cleared load is within 13% of the FE model on the first rebound.

Figure 13: FE and SDOF response under different loading conditions for a 1 m square cladding panel

$R_u/F_{e,max}$	t_d/T	z_{max} (mm)			
		LS-DYNA	Clearing	Exponential	Triangular
0.094	0.116	15.3	17.3	28.1	47.7
		% diff.	13	83	211

Table 3: Maximum response for FE and SDOF model from numerical analysis and percentage difference between FE and SDOF displacements

It is possible to determine the peak displacement without the need for numerical analysis, simply by using the response spectra provided in Figure 8. Taking $R_u/F_{e,max}$ and t_d/T as 0.10 and 0.12 respectively, the peak displacement for $Z/H = 8$ can be read off Figure 8(c) to give $z_{max} = 1.7z_E$, which compares well with $1.53z_E$ determined from the FE analysis. If clearing is neglected and the peak displacement under the exponential load is read from Figure 8(a), the peak displacement would be estimated at $2.6z_E$. If the loading is further simplified as a triangular load with no provision for clearing or the negative phase, the peak displacement would be estimated from Figure 3 as $5.0z_E$. These correspond to over-predictions of 70% and 230% respectively, demonstrating the need to take blast wave clearing into account, especially during the early stages of design.

Peak displacements obtained using the graphical response spectra method are summarised in Table 4.

$R_u/F_{e,max}$	t_d/T	z_{max}/z_E			
		LS-DYNA	Clearing Fig. 8(c)	Exponential Fig. 8(a)	Triangular Fig. 3
0.1	0.12	1.53	1.7	2.6	5.0
		% diff.	11	70	230

Table 4: Normalised maximum response for FE and SDOF model using graphical method and percentage difference between FE and SDOF displacements

7. Summary and Conclusions

The objective of this study has been to quantify the effect of blast wave clearing on elastic-plastic systems via rigorous analysis of elastic-plastic one degree systems.

The equivalent Single-Degree-of-Freedom method is often favoured for use in preliminary design because of its non-specialist requirements, low computational cost and relatively few input parameters. Literature guidance [7, 9] recommends using response spectra based on elastic-perfectly plastic SDOF response to a linearly decaying blast load. Gantes and Pnevmatikos [13] provide response spectra for more realistic exponential loads, however neither method takes clearing into account.

In this study, the dynamic equation of motion is solved using explicit dynamics for equivalent SDOF systems. Normalised target sizes of Z/H = 0, 4, 8 and 16 are subjected to cleared blast loads determined using Hudson clearing predictions [27] with the equivalent SDOF force calculated using the spatial load factor, K_S, developed in [20].

Blast wave clearing generally serves to reduce the peak displacement of the target, particularly when the magnitude of the load is large relative to the resistance of the target, and the load duration is large relative to the response time of the target. It has also been shown that neglecting clearing may be unsafe for certain configurations of target size, mass, stiffness and elastic resistance. It is therefore important that blast wave clearing is considered at all stages of blast resistant design.

A numerical example has shown that the response spectra can be used to predict the peak response of a finite target to within 11% of an explicit finite element model, compared to a 230% over-prediction when simplifying the load as a triangular pulse and reading off the response spectra provided in current design guidance.

The results presented in this article can be used with confidence as a first means for predicting the likely damage a target will sustain when subjected to an explosive load.

[1] Børvik T, Hanssen A, Langseth M, Olovsson L. Response of structures to planar blast loads – A finite element engineering approach. Computers & Structures 2009;87(9-10):507–20.

[2] Chafi MS, Karami G, Ziejewski M. Numerical analysis of blast-induced wave propagation using FSI and ALE multi-material formulations. International Journal of Impact Engineering 2009;36(10-11):1269–75.

[3] Neuberger A, Peles S, Rittel D. Scaling the response of circular plates subjected to large and close-range spherical explosions. Part I: Air-blast loading. International Journal of Impact Engineering 2007;34(5):859–73.

[4] Zakrisson B, Wikman B, Häggblad H. Numerical simulations of blast loads and structural deformation from near-field explosions in air. International Journal of Impact Engineering 2011;38(7):597–612.

[5] Tai Y, Chu T, Hu H, Wu J. Dynamic response of a reinforced concrete slab subjected to air blast load. Theoretical and Applied Fracture Mechanics 2011;56(3):140–7.

[6] Wang W, Zhang D, Lu F, Wang Sc, Tang F. Experimental study and numerical simulation of the damage mode of a square reinforced concrete slab under close-in explosion. Engineering Failure Analysis 2013;27:41–51.

[7] US DoD (Department of Defence) . Structures to resist the effects of accidental explosions. US DoD, Washington DC, USA, UFC-3-304-02; 2008.

[8] Biggs J. Introduction to structural dynamics. McGraw-Hill, NY, USA; 1964.

[9] Cormie D, Mays G, Smith P. Blast effects on buildings, 2nd ed. Thomas Telford, London, UK; 2009.

[10] U.S. Army Corps of Engineers. Methodology manual for the Single-Degree-of-Freedom Blast Effects Design Spreadsheets (SBEDS), PDC TR-06-01; 2008.

[11] Kingery C, Bulmash G. Airblast parameters from tnt spherical air burst and hemispherical surface burst. Tech. Rep. ARBL-TR-02555; U.S Army BRL, Aberdeen Proving Ground, MD, USA; 1984.

[12] Hyde D. Conventional Weapons Program (ConWep). U.S Army Waterways Experimental Station, Vicksburg, MS, USA; 1991.

[13] Gantes C, Pnevmatikos N. Elastic-plastic response spectra for exponential blast loading. International Journal of Impact Engineering 2004;30(3):323–43.

[14] Tyas A, Warren J, Bennett T, Fay S. Prediction of clearing effects in far-field blast loading of finite targets. Shock Waves 2011;21(2):111–9.

[15] Rickman DD, Murrell DW. Development of an improved methodology for predicting airblast pressure relief on a directly loaded wall. Journal of Pressure Vessel Technology 2007;129(1):195–204.

[16] Rose TA, Smith PD, May JH. The interaction of oblique blast waves with buildings. Shock Waves 2006;16(1):35–44.

[17] Smith PD, Rose TA, Saotonglang E. Clearing of blast waves from building facades. Proceedings of the Institution of Civil Engineers - Structures and Buildings 1999;134(2):193–9.

[18] Ballantyne GJ, Whittaker AS, Dargush GF, Aref AJ. Air-blast effects on structural shapes of finite width. Journal of Structural Engineering 2010;136(2):152 –9.

[19] Rose T, Smith P. An approach to the problem of blast wave clearing on finite structures using empirical procedures based on numerical calculations. In: 16th Symposium on the Military Aspects of Blast and Shock (MABS16). Oxford, UK; 2000, p. 113–20.

[20] Rigby SE, Tyas A, Bennett T. Single-degree-of-freedom response of finite targets subjected to blast loading - the influence of clearing. Engineering Structures 2012;45:396–404.

[21] Rigby SE, Tyas A, Bennett T, Warren JA, Fay S. Clearing effects on plates subjected to blast loads. Engineering and Computational Mechanics 2013;166(3):140–8.

[22] Baker WE. Explosions in air. University of Texas Press, Austin, TX, USA; 1973.

[23] Teich M, Gebbeken N. The influence of the underpressure phase on the dynamic response of structures subjected to blast loads. International Journal of Protective Structures 2010;1(2):219–34.

[24] Krauthammer T, Altenberg A. Negative phase blast effects on glass panels. International Journal of Impact Engineering 2000;24(1):1 – 17.

19

[25] Naval Facilities Engineering Command (NavFac). Blast resistant structures, NFE DM 2-08; 1986.

[26] Shi Y, Hao H, Li ZX. Numerical simulation of blast wave interaction with structure columns. Shock Waves 2007;17(1-2):113–33.

[27] Hudson C. Sound pulse approximations to blast loading (with comments on transient drag). Tech. Rep. SC-TM-191-55-51; Sandia Corporation, MD, USA; 1955.

[28] Hallquist JO. LS-DYNA Theory Manual. Livermore Software Technology Corporation, CA, USA; 2006.

Appendix A. Response spectra for Z = 2, 4 and 16 m/kg$^{1/3}$

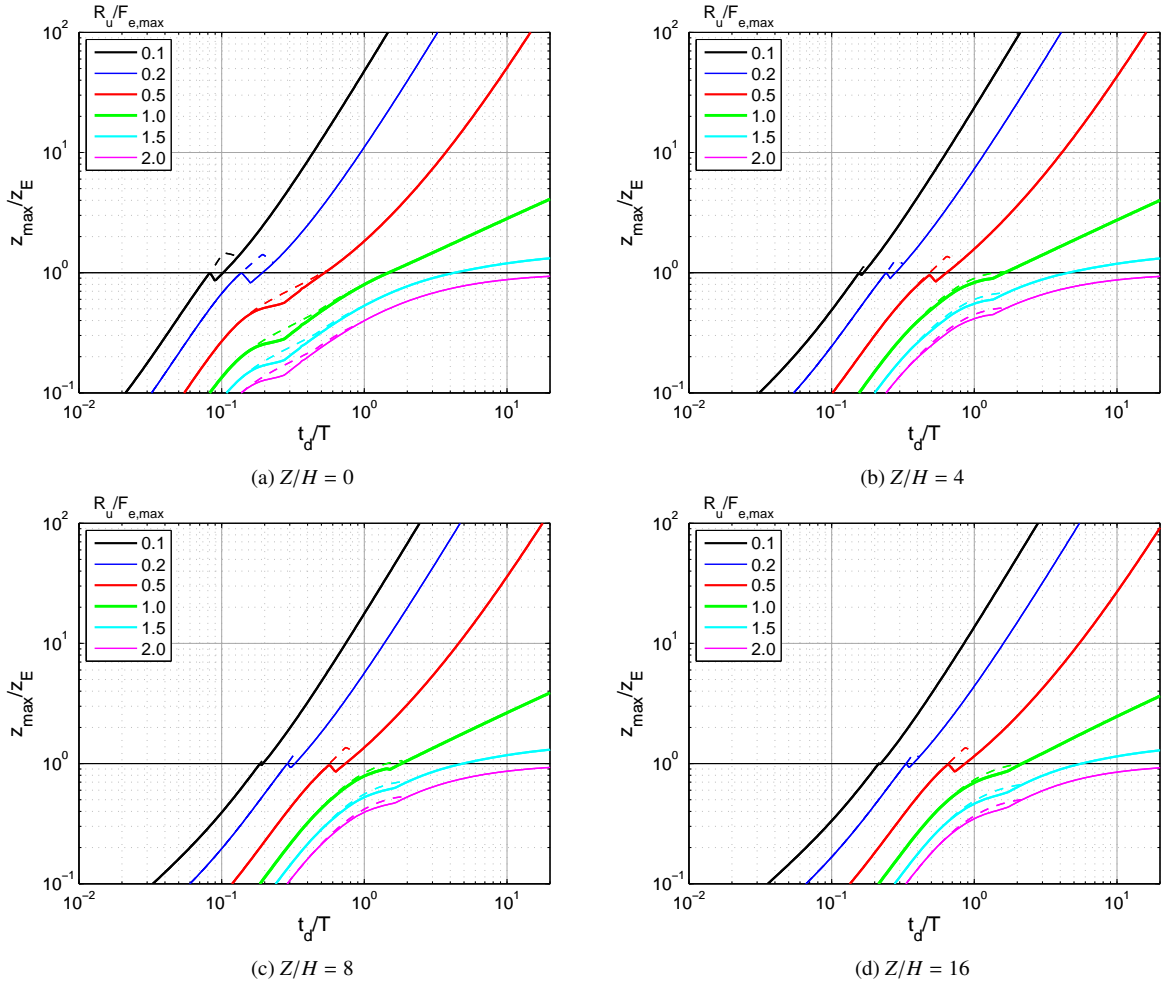Figures A.1, A.2 and A.3 show elastic-plastic response spectra for Z = 2, 4 and 16 m/kg$^{1/3}$ respectively.

Figure A.1: Response spectra for $Z = 2$ m/kg$^{1/3}$. Dashed lines indicate regions where the peak displacement is in rebound
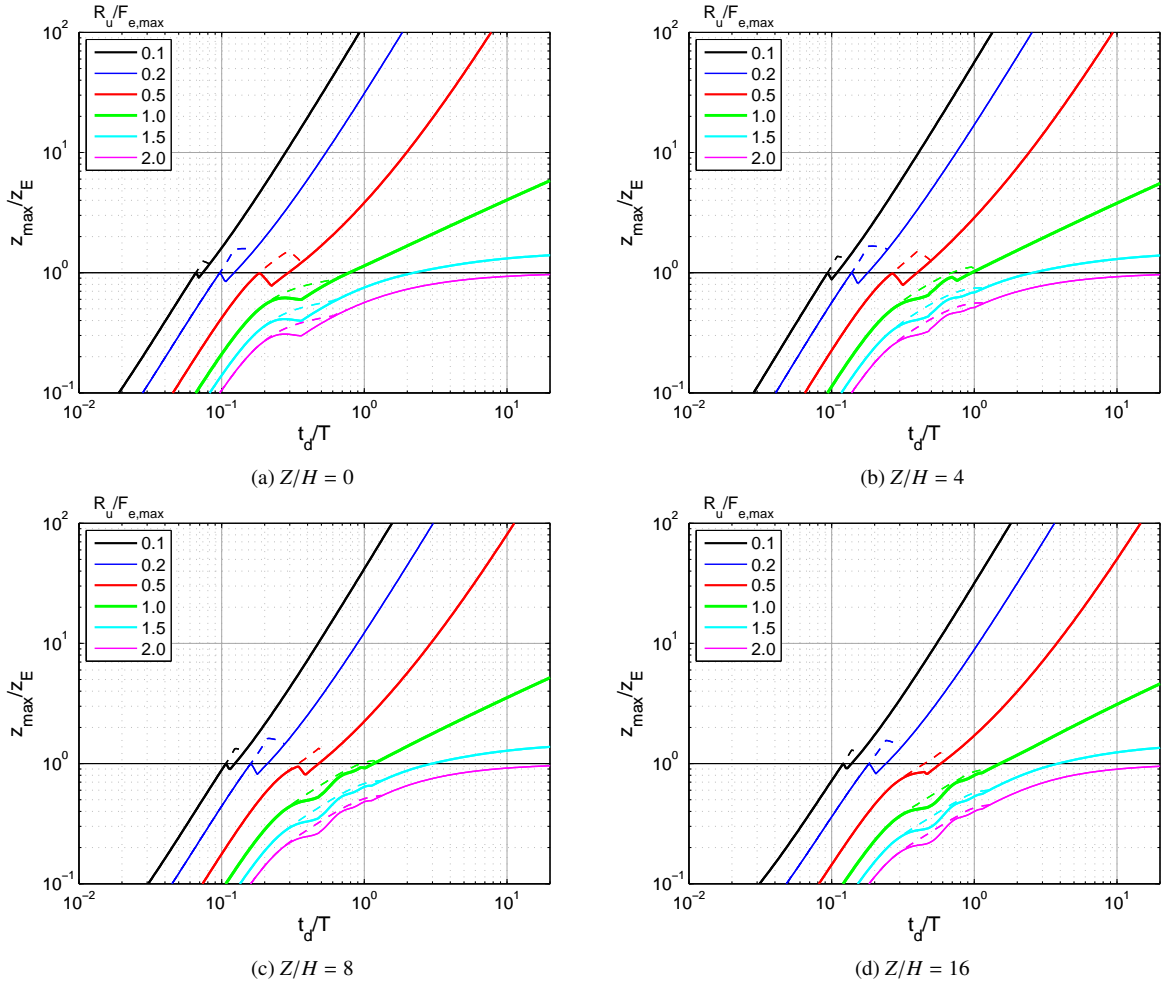
Figure A.2: Response spectra for $Z = 4$ m/kg$^{1/3}$. Dashed lines indicate regions where the peak displacement is in rebound
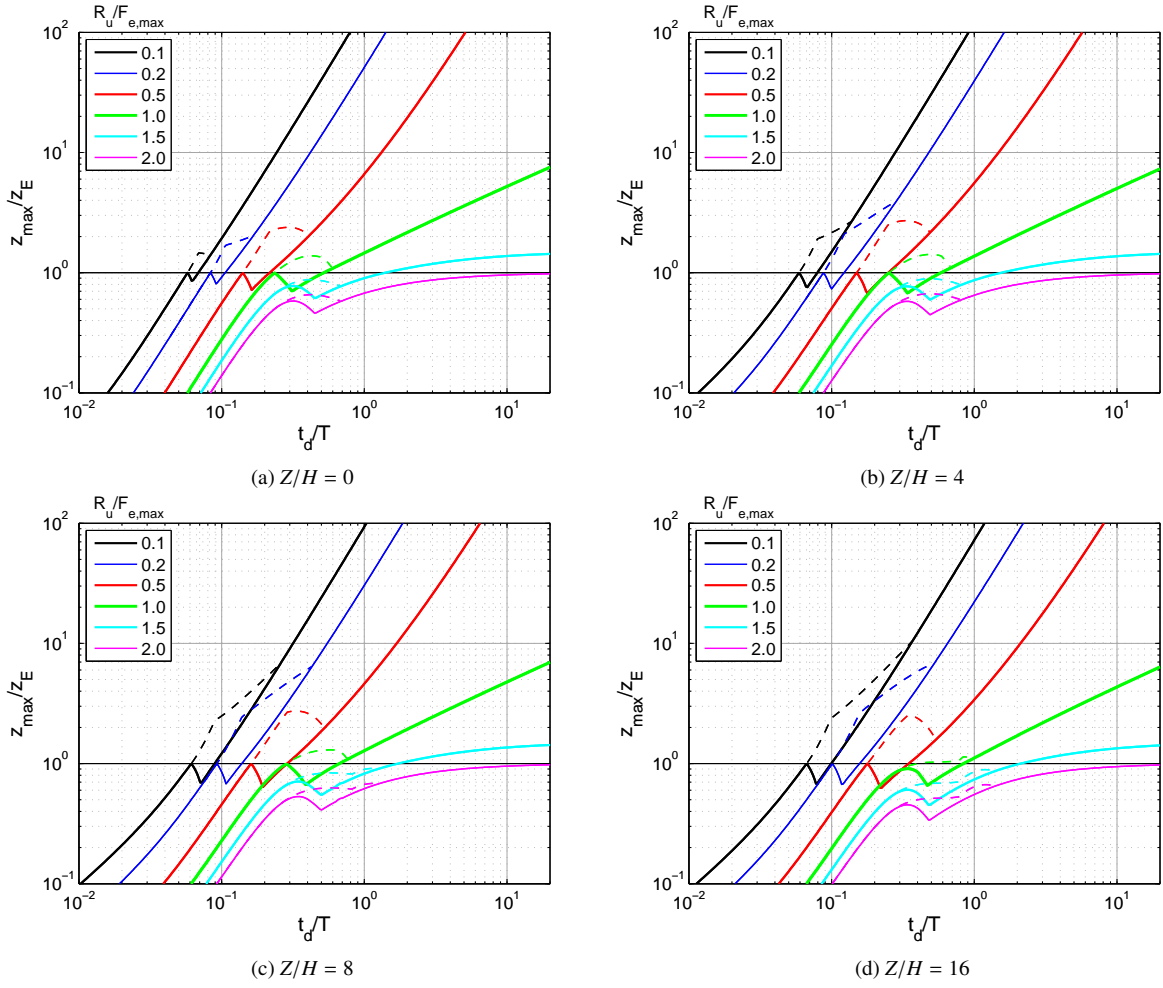
(a) $Z/H = 0$

(b) $Z/H = 4$

(c) $Z/H = 8$

(d) $Z/H = 16$

Figure A.3: Response spectra for $Z = 16$ m/kg$^{1/3}$. Dashed lines indicate regions where the peak displacement is in rebound